Original Article

Cx36-Mediated Coupling Reduces β-Cell Heterogeneity, Confines the Stimulating Glucose Concentration Range, and Affects Insulin Release Kinetics

Stephan Speier,[1] Asllan Gjinovci,[2] Anne Charollais,[2] Paolo Meda,[2] and Marjan Rupnik[1]

We studied the effect of gap junctional coupling on the excitability of β-cells in slices of pancreas, which provide a normal environment for islet cells. The electrophysiological properties of β-cells from mice (C57Bl/6 background) lacking the gap junction protein connexin36 ($Cx36^{-/-}$) were compared with heterozygous ($Cx36^{+/-}$) and wild-type littermates ($Cx36^{+/+}$) and with frequently used wild-type NMRI mice. Most electrophysiological characteristics of β-cells were found to be unchanged after the knockout of Cx36, except the density of Ca^{2+} channels, which was increased in uncoupled cells. With closed ATP-sensitive K^+ (K_{ATP}) channels, the electrically coupled β-cells of $Cx36^{+/+}$ and $Cx36^{+/-}$ mice were hyperpolarized by the membrane potential of adjacent, inactive cells. Additionally, the hyperpolarization of one β-cell could attenuate or even stop the electrical activity of nearby coupled cells. In contrast, β-cells of $Cx36^{-/-}$ littermates with blocked K_{ATP} channels rapidly depolarized and exhibited a continuous electrical activity. Absence of electrical coupling modified the electrophysiological properties of β-cells consistent with the reported increase in basal insulin release and altered the switch on/off response of β-cells during an acute drop of the glucose concentration. Our data indicate an important role for Cx36-gap junctions in modulating stimulation threshold and kinetics of insulin release. ***Diabetes*** **56:1078–1086, 2007**

Pancreatic β-cells express gap junctions (1), and electrophysiological (2) and dye microinjection approaches (3) have indicated that these structures provide for coupling, i.e., for the exchange of ions and small metabolites between β-cells. Coupling of β-cells has been shown to improve insulin synthesis and secretion, whereas uncoupling leads to altered β-cell function (4). Furthermore, the property of islets of Langerhans to function as a syncytium in terms of electrical bursting and Ca^{2+} signals has also been attributed to coupling (5). Thus, gap junctions are considered to provide one of the micro-anatomical bases for appropriate glucose-induced insulin release (6).

In 2000, Serre-Beinier et al. (7) revealed that gap junctions of pancreatic β-cells are made of the Connexin36 (Cx36) protein, and more recent data indicate that, in contrast to most other cell types, β-cells do not appear to express other connexin species (8). Studies on the MIN6 and INS-1E cell lines and on primary β-cells have revealed that sizable alterations in the levels of Cx36 expression are associated with impaired secretory response to glucose (9–11). Recently, a study on mutant mice that do not express Cx36 ($Cx36^{-/-}$) demonstrated that this protein has a physiological impact on insulin secretion under in vivo conditions (12). Thus, lack of Cx36 resulted in the loss of the normally coordinated Ca^{2+} signals between β-cells and in the regularly pulsatile release of insulin from isolated islets. Additionally, islets of mice lacking gap junctional coupling featured a significantly higher basal release of insulin in the presence of substimulatory glucose concentrations (12).

To elucidate the mechanism leading to these changes, we have now investigated the electrophysiological properties of β-cells of Cx36-deficient mice (13), in comparison with those of heterozygous and wild-type littermates. For this purpose, we have used a pancreatic tissue slice preparation (14), which allows for the evaluation of the excitability of β-cells in their native, in situ environment. The findings were also compared with those made, under similar experimental conditions, in mice of the NMRI strain, which have been used so far in most electrophysiological studies of β-cells.

RESEARCH DESIGN AND METHODS

Preparation of pancreatic slices. Experiments compared Cx36-deficient mice with a C57Bl/6 background ($Cx36^{-/-}$) with their heterozygous ($Cx36^{+/-}$) and wild-type littermates ($Cx36^{+/+}$) (13). They also evaluated NMRI mice, inasmuch as this strain of mice has been the most characterized in terms of β-cell electrophysiology. All experiments were performed according to the animal care regulations of our universities and states. Genotyping was performed by PCR analysis and Southern blot hybridization, as reported (13). Mice were killed by cervical dislocation, and pancreas slices were prepared as described previously (14). During and after slicing, the tissue was kept in an ice-cold extracellular solution, continuously bubbled with carbogen. At least 30 min before the experiment, the slices were transferred to a carbogen-bubbled extracellular solution at 32°C. β-Cells were studied within undamaged islets of Langerhans located close to the surface of the slices.

Electrophysiology. The perfusion chamber was mounted on an upright Eclipse E600FN microscope (Nikon, Tokyo, Japan) equipped with a ×60, 0.9 N.A. objective. During patch-clamp experiments, the slices were continuously superfused with a carbogen-bubbled extracellular solution (32°C, 1.5 ml/min).

Membrane potential and whole-cell currents were recorded under a standard whole-cell configuration. The holding potential during voltage-clamp recording was −70 mV. Data were acquired at 20 kHz using a double EPC9

From the [1]Neuroendocrinology, European Neuroscience Institute Göttingen, Göttingen, Germany; and the [2]Department of Cell Physiology and Metabolism, University of Geneva, Genève, Switzerland.

Address correspondence and reprint requests to Stephan Speier, The Rolf Luft Center for Diabetes Research, Department of Molecular Medicine and Surgery, Karolinska Institutet, Karolinska University Hospital L1, Stockholm, Sweden. E-mail: stephan.speier@ki.se.

Received for publication 19 February 2006 and accepted in revised form 15 December 2006.

Cx36, connexin36; K_{ATP} channel, ATP-sensitive K^+ channel.

DOI: 10.2337/db06-0232

amplifier (HEKA Electronik, Lambrecht/Pfalz, Germany) with PULSE8.74 and PATCHMASTER 2.0 software and stored on a PC computer. The offset of the HEKA amplifier, observed under high input resistance conditions, was not corrected. Whole-cell conductance, reflecting primarily ATP-sensitive K^+ (K_{ATP}) channel and Cx36 channel activity, was read as a slope of a current-voltage curve between −100 and −60 mV (15).

Patch pipettes with a resistance of 2–4 MΩ, measured with standard intracellular solution, were prepared from borosilicate glass capillaries (Harvard Apparatus, Holliston, U.K.) using a P-97 puller (Sutter Instruments). The standard extracellular medium consisted of 125 mmol/l NaCl, 2.5 mmol/l KCl, 26 mmol/l $NaHCO_3$, 1.25 mmol/l NaH_2PO_4, 2 mmol/l Na pyruvate, 0.25 mmol/l ascorbic acid, 3 mmol/l *myo*-inositol, 6 mmol/l lactic acid, 1 mmol/l $MgCl_2$, and 2 mmol/l $CaCl_2$. The glucose concentration during incubations and experiments was 3 mmol/l, except when differently indicated. The pipette filling solution contained 150 mmol/l KCl, 4 mmol/l NaCl, 10 mmol/l HEPES, 2 mmol/l $MgCl_2$, 0.05 mmol/l EGTA (pH 7.2 with KOH), and ATP as indicated. For the recording of Ca^{2+} currents, outward K^+ currents were suppressed by including 20 mmol/l tetraethylammonium chloride and by replacing KCl with 130 mmol/l CsCl in the pipette solution. By dialyzing β-cells localized deeply within islets of Langerhans with high ATP concentrations, we were able to limit closure of K_{ATP} channels to one patched cell only within the time frame of the experiment. The K_{ATP} channel blocker tolbutamide (100 μmol/l) was added to the extracellular medium to block K_{ATP} channels in the entire slice, to stimulate electrical activity, and to evaluate the residual conductance after inhibition of K_{ATP} channels.

Insulin secretion kinetics. Perfusion of the whole pancreas was performed in situ, as reported previously (16). The pancreas was perfused at 37°C with 1 ml/min, a flux that was maintained in all mice using a pressure column pump (16). The perfusate contained 1.4 mmol/l glucose at basal and 16.4 mmol/l glucose at stimulated conditions, each applied for 15 min. Throughout the test period (15 min basal, 15 min stimulation, and 15 min basal), the effluent was sampled at 30-s intervals. The decay in insulin release induced by the decrease in glucose concentration from 16.4 to 1.4 mmol/l was normalized to the steady-state level of insulin release at the end of the 16.4 mmol/l glucose stimulation.

Data analysis. Data analysis was done using the PULSEFIT 8.74 and FITMASTER 2.11 (HEKA Electronik), Matview (Matlab Pulse extension; Wise Technologies, Ljubljana, Slovenia), and SigmaPlot v9.0 software (Systat Software). The activation and deactivation parameters of the K^+ and Ca^{2+} currents were calculated using FITMASTER software (HEKA Electronik). Data were displayed as mean ± SE, with n indicating the number of cells analyzed. Statistical significance was determined by one-way ANOVA or Student's t test and was considered significant at $P < 0.05$.

RESULTS

Electrophysiology allowed for β-cell comparison between Cx36 and NMRI mice. The capacitance of β-cells was comparable in $Cx36^{+/+}$ (6.9 ± 0.3 picofarads [pF], n = 45), $Cx36^{+/-}$ (7.3 ± 0.3 pF, n = 23), and $Cx36^{-/-}$ mice (6.6 ± 0.1 pF, n = 79), indicating a comparable size of β-cells. Thus, the capacitance value could be used as a first parameter to help distinguish β-cells from non–β-cells (15,17), inasmuch as non–β-cells are smaller in size than β-cells. The membrane potential of the conditioning pulse (V_h) that reduced by 50% the amplitude of the Na^+ current was also comparable in the β-cells of all animals studied (−100 ± 1 mV, n = 6; −98 ± 1 mV, n = 6; and −100 ± 1 mV, n = 6, in $Cx36^{+/+}$, $Cx36^{+/-}$, and $Cx36^{-/-}$ mice, respectively). These potentials are similar to those previously published for β-cells (17) and notably different from those reported for non–β-cells (18,19). Therefore, we were able to use V_h as a second parameter to distinguish β-cells from non–β-cells.

β-Cells of control $Cx36^{+/+}$ mice on a C57Bl/6 background displayed most of the electrophysiological characteristics previously reported in control NMRI mice (14). In particular, the two strains of animals featured a similar capacitance of β-cells (6.9 ± 0.3 pF, n = 45, and 6.9 ± 0.1 pF, n = 266, in $Cx36^{+/+}$ and NMRI mice, respectively) and a comparable membrane potential of the conditioning pulse V_h (−100 ± 1 mV, n = 6, and −103 ± 1 mV, n = 4, in $Cx36^{+/+}$ and NMRI mice, respectively). The two mouse strains also showed a sizable residual conductance after blockade of K_{ATP} channels (Fig. 1*A* and *B*). However, the level of this conductance, which is mainly attributable to gap junctions, was significantly different in the two strains of mice (1.2 ± 0.1 nS, n = 8, and 2.1 ± 0.3 nS, n = 8, in $Cx36^{+/+}$ and NMRI mice, respectively). Also, when measured without ATP in the pipette solution, K_{ATP} channels developed a maximal conductance of 2.4 ± 0.2 nS/pF (n = 20) in the β-cells of NMRI mice but a significantly higher conductance (3.3 ± 0.3 nS/pF, n = 14; $P < 0.015$) in those of $Cx36^{+/+}$ mice, which had a C57Bl/6 background (Fig. 1*C*). The density of Ca^{2+} currents was also similar in the

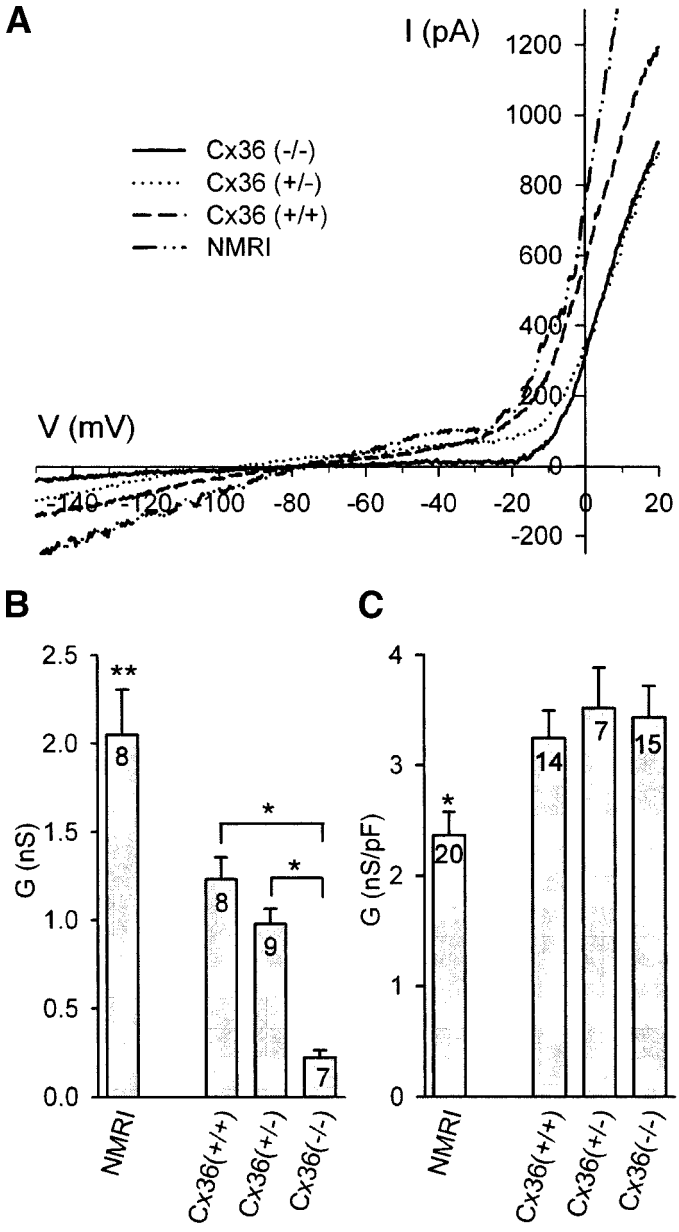

FIG. 1. Residual whole-cell conductance and K_{ATP}-channel density of β-cells from NMRI, $Cx36^{+/+}$, $Cx36^{+/-}$, and $Cx36^{-/-}$ mice (latter three mice have a C57Bl/6 background). *A*: Representative traces of current responses to a voltage ramp, after K_{ATP}-channel closure by 5 mmol/l intracellular ATP and extracellular application of 100 μmol/l tolbutamide. *B*: Statistics of the residual conductance measured as the slope of the current response between −100 and −60 mV. *C*: Maximal K_{ATP}-channel conductance after dialysis in the absence of ATP. *P < 0.05, **P < 0.05 vs. value of $Cx36^{+/+}$ mice.

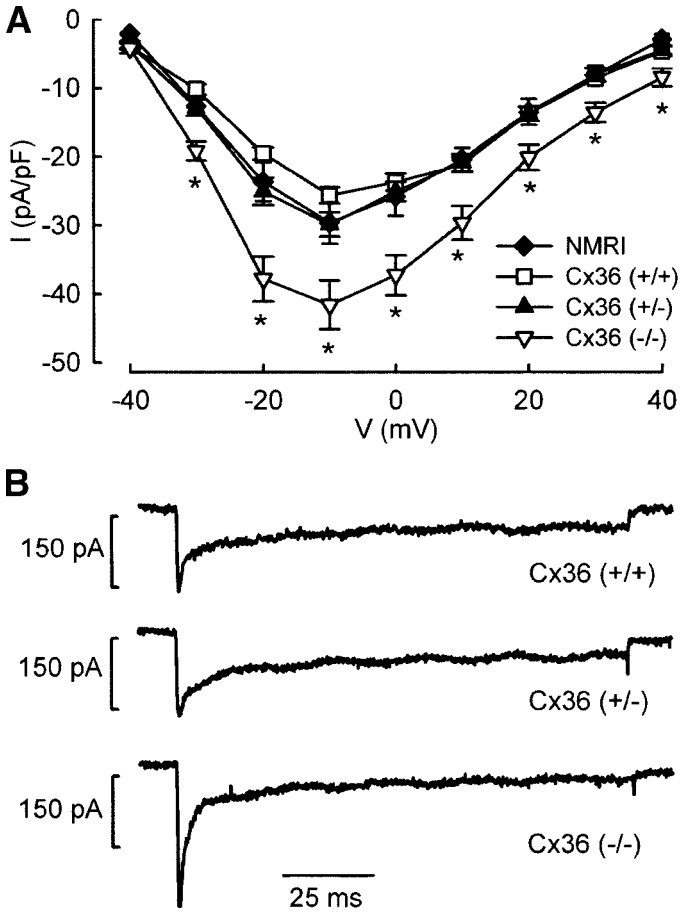

FIG. 2. *A*: Current-voltage relation of Ca^{2+} channels (n = 11–13) of β-cells from NMRI, $Cx36^{+/+}$, $Cx36^{+/-}$, and $Cx36^{-/-}$ mice (latter three on a C57Bl/6 background). *B*: Representative traces of Ca^{2+} currents of β-cells from $Cx36^{+/+}$, $Cx36^{+/-}$, and $Cx36^{-/-}$ mice in response to a voltage step depolarization to −10 mV from a holding potential of −70 mV. *Significant differences (P < 0.05).

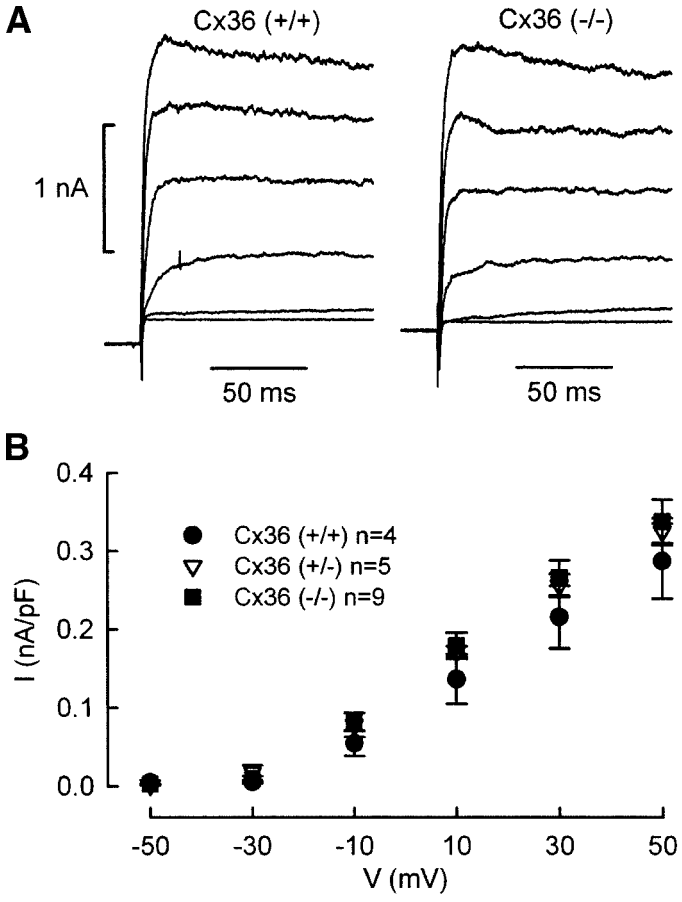

FIG. 3. K^+ currents in coupled and noncoupled β-cells. *A*: Representative current traces of $Cx36^{+/+}$ and $Cx36^{-/-}$ β-cells in response to step depolarizations between −50 and +50 mV from a holding potential of −150 mV. *B*: Current-voltage relationship of peak outward current in β-cells from $Cx36^{+/+}$, $Cx36^{+/-}$, and $Cx36^{-/-}$ mice.

two strains (Fig. 2*A*). Maximal peak Ca^{2+}-current density was 30 ± 3 picoamperes [pA]/pF and 26 ± 1 pA/pF in NMRI (n = 11) and $Cx36^{+/+}$ mice on a C57Bl/6 background (n = 11), respectively.

β-Cells lacking Cx36 were uncoupled and showed a different excitability than cells expressing the connexin. To determine the contribution of gap junction channels to the measured whole-cell conductance, the cell cytosol was exposed, via the patched pipette, to 5 mmol/l ATP, while the slice was perfused with 100 μmol/l tolbutamide. This treatment results in the closure of almost all K_{ATP} channels, which, under resting conditions, account for the major part of the whole β-cell conductance (20). Under these conditions, the residual conductance is attributable mainly to gap junction channels. Figure 1*A* shows representative current traces of β-cells from $Cx36^{+/+}$, $Cx36^{+/-}$, and $Cx36^{+/-}$ mice in response to a voltage ramp from −150 to 50 mV, where whole-cell conductance can be measured as the slope of the current trace between −100 and −60 mV. The junctional conductance was 1.2 ± 0.1 nS (n = 8) and 1.0 ± 0.1 nS (n = 9) in $Cx36^{+/+}$ and $Cx36^{+/-}$ mice, respectively (Fig. 1*B*), i.e., in animals whose β-cells were linked by Cx36-made gap junctions (12). In contrast, this conductance was markedly decreased (P < 0.001) in $Cx36^{-/-}$ mice that lacked β-cell gap junctions. The residual level of conductance (0.2 ± 0.05 nS, n = 7; Fig. 1*B*) observed in these animals was similar to that (0.22 ± 0.06 nS, n = 13) measured in isolated primary β-cells, after closure of K_{ATP} channels (15). Despite the lack of coupling, we did not observe an increased channel noise in current recordings from $Cx36^{-/-}$ β-cells (Figs. 1–3).

Next, we evaluated whether loss of Cx36 channels altered the density of other types of channels within the β-cell membrane. Comparing $Cx36^{+/+}$, $Cx36^{+/-}$, and $Cx36^{-/-}$ mice, we found no difference in terms of the Na^+-current inactivation pattern, the Na^+-current density (data not shown), and the K_{ATP}-channel density (Fig. 1*C*). Also, the current density and voltage dependence of K^+ channels evoked by 200-ms depolarizations of membrane potential between −50 and +50 mV, starting from a holding potential of −150 mV, were similar in $Cx36^{+/+}$, $Cx36^{+/-}$, and $Cx36^{-/-}$ mice (Fig. 3). At +50 mV, the peak amplitudes averaged 287 ± 48 (n = 4), 325 ± 17 (n = 5), and 338 ± 28 pA/pF (n = 9) in $Cx36^{+/+}$, $Cx36^{+/-}$, and $Cx36^{-/-}$ mice, respectively (Fig. 3*B*). Additionally, the activation of the K^+ current, described by n^4 kinetics, showed no significant difference. The time constant of activation (τ_n) at depolarizations to +50 mV was 1.31 ± 0.07, 1.23 ± 0.12, and 1.31 ± 0.14 ms in $Cx36^{+/+}$, $Cx36^{+/-}$, and $Cx36^{-/-}$ mice, respectively (data not shown). Figure 2*A* displays the current voltage relation of Ca^{2+}-current densities, as evaluated after a 100-ms-step depolarization protocol, going from −70 mV to voltages between −40 and +40 mV. This protocol revealed significantly higher Ca^{2+}-

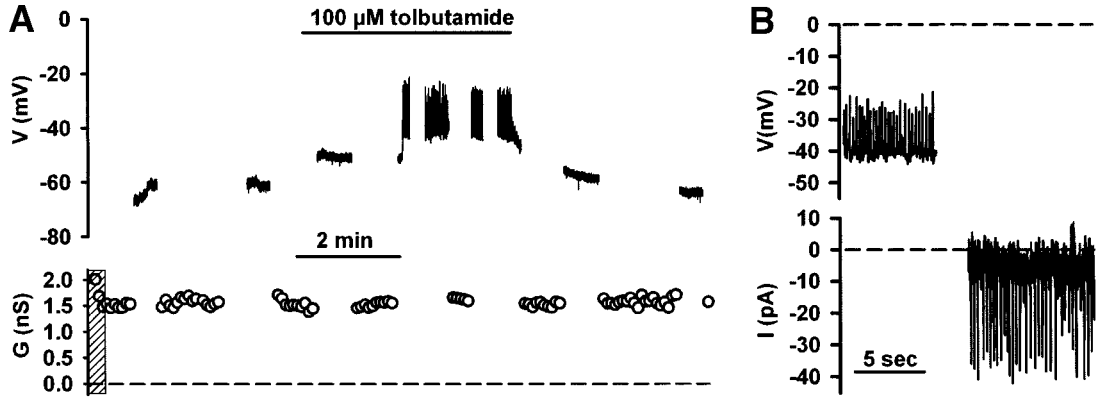

FIG. 4. Excitability of β-cells of Cx36$^{+/+}$ mice. *A*: Membrane potential (top trace) and whole-cell conductance (bottom trace) as a result of intracellular dialysis of 5 mmol/l ATP and extracellular application of 100 μmol/l tolbutamide. Gaps in the recording indicate application of voltage protocols to assess channel properties. *B*: Currents recorded at −50 mV (bottom trace) during electrical activity (top trace).

current densities in β-cells of Cx36$^{-/-}$ than in those of both Cx36$^{+/-}$ and Cx36$^{+/+}$ littermates. The maximal peak Ca^{2+}-current density in β-cells was 26 ± 1 (n = 11), 30 ± 2 (n = 11), and 41 ± 4 pA/pF (n = 13) in Cx36$^{+/+}$, Cx36$^{+/-}$, and Cx36$^{-/-}$ mice, respectively. In contrast to the current density, the voltage dependence of the Ca^{2+}-current traces showed no obvious difference (Fig. 2*A*). Furthermore, the inactivation of the Ca^{2+} current, which was best fit by a double exponential function, was not significantly different (Fig. 2*B*). The inactivation constants (τ_1 and τ_2) of the current at peak stimulation were evaluated as 2.71 ± 0.67 and 39.53 ± 11.73, 3.92 ± 0.57 and 40.14 ± 5.73, and 2.33 ± 0.74 and 40.80 ± 11.83 in Cx36$^{+/+}$, Cx36$^{+/-}$, and Cx36$^{-/-}$ mice, respectively (data not shown). However, we cannot fully exclude a variation in the contribution of different Ca^{2+}-channel subtypes, which would require a more detailed pharmacological study.

To study the effect of gap junctions on the electrical activity of β-cells, we recorded the changes in membrane potential and whole-cell conductance during stimulation. During dialysis of β-cells of Cx36$^{+/+}$ mice with 5 mmol/l ATP, which was added to the solution filling the patch-pipette, most K_{ATP} channels closed within a few tens of seconds, and a sizable and stable residual conductance was measured (Fig. 4*A*, bottom trace). On the average, this residual conductance was 1.6 ± 0.3 nS (n = 5), which is not significantly different from the residual conductance after an additional application of tolbutamide. Under such conditions, membrane potential depolarized only to levels (−70 ± 7 mV) below the threshold potential for stimulation of electrical activity (n = 5). Additional application of 100 μmol/l tolbutamide, via the extracellular bath solution, further depolarized the membrane potential up to a statistically significant higher level (−40 ± 2 mV, P = 0.002) and induced a typical electrical activity of β-cells, with spikes peaking between −30 and −20 mV (Fig. 4*A* and *B*, *upper trace*). In Cx36$^{+/+}$ mice, the spikes had a frequency of 5.5 ± 0.8 Hz with a mean and maximal amplitude of 17.1 ± 0.8 and 24.7 ± 1.3 mV, respectively (n = 8) (Table 1). After washout of tolbutamide, the membrane potential returned to the lower, initial levels. Notably, whole-cell conductance did not change during both the application and the washout of the sulfonylurea (Fig. 4*A*, *bottom trace*). During the application of tolbutamide we did not detect any second-lasting bursts of electrical activity in Cx36$^{+/+}$ β-cells. To reveal the origin of the potential changes, we blocked the contribution of voltage-activated channels, including L-type Ca^{2+} channels, by clamping β-cells at −50 mV. These conditions revealed non–voltage-activated channels in the plasma membrane of the patched β-cell to participate in its electrical activity. As shown in the bottom trace of Fig. 4*B*, inward currents were observed under voltage-clamp conditions. These incoming currents mirrored the frequency of the spiking activity recorded in electrically active β-cells (Fig. 4*B*, *upper trace*), indicating that they drive the membrane potential changes recorded under current-clamp conditions. This lack of voltage dependence has been previously reported to be a characteristic parameter of Cx36 channels (12,21–23).

Under the same experimental conditions, β-cells of Cx36$^{+/-}$ mice behaved as described for wild-type, Cx36$^{+/+}$ littermates (Fig. 5) and featured a similar spike frequency (5.2 ± 0.8 Hz [n = 5] and 5.5 ± 0.8 Hz [n = 8]), mean amplitude (16.0 ± 1.6 mV [n = 5] and 17.1 ± 0.8 mV [n = 8]), and maximal amplitude (22.0 ± 1.5 mV [n = 5] and 24.7 ± 1.3 mV [n = 8]; Table 1). In contrast, β-cells of Cx36$^{-/-}$ mice revealed a quite different behavior. Thus, whereas after intracellular exposure to ATP, their K_{ATP} channels closed, with a time profile similar to that observed in β-cells expressing Cx36 (Fig. 6*A*, *inset*), a minimal conductance was observed, consistent with the lack of gap junction channels. On the average, this small conductance was 0.2 ± 0.05 nS (n = 6). Furthermore, the depolarization induced by reducing the K_{ATP} conductance by ATP dialysis was significantly larger in the uncoupled Cx36$^{-/-}$ β-cells than in the coupled Cx36$^{+/+}$ and Cx36$^{+/-}$ cells (P < 0.05). Thus, uncoupled β-cells readily reached the threshold potential for activation of electrical activity (−41 ± 2 mV, n = 6), leading to the generation of spikes peaking between −10 and 0 mV. Although the spiking frequency of Cx36$^{-/-}$ mice (5.3 ± 0.5 Hz) was similar to that recorded from Cx36$^{+/+}$ and Cx36$^{+/-}$ β-cells, mean

TABLE 1
Spiking characteristics of β-cells from Cx36$^{+/+}$, Cx36$^{+/-}$, and Cx36$^{-/-}$ mice

	n	Mean spiking frequency (Hz)	Spike amplitude (mV)	
			Mean	Maximal
Cx36$^{+/+}$	8	5.5 ± 0.8	17.1 ± 0.8	24.7 ± 1.3
Cx36$^{+/-}$	5	5.2 ± 0.8	16.0 ± 1.6	22.0 ± 1.5
Cx36$^{-/-}$	11	5.3 ± 0.5	27.3 ± 1.7*	40.9 ± 2.3†

Data are mean ± SE. *P < 0.002. †P < 0.001.

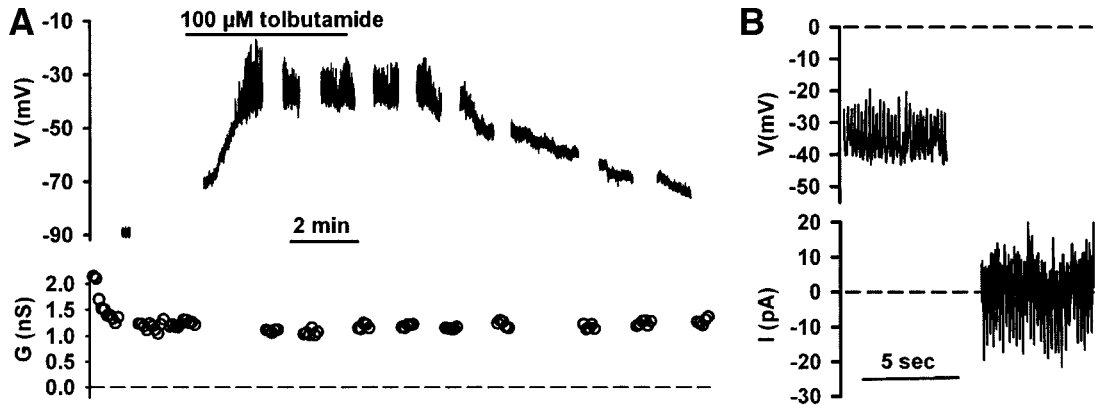

FIG. 5. Excitability of β-cells of Cx36$^{+/-}$ mice. *A*: Membrane potential (top trace) and whole-cell conductance (bottom trace) as a result of intracellular dialysis of 5 mmol/l ATP and extracellular application of 100 µmol/l tolbutamide. *B*: Currents recorded at −50 mV (bottom trace) during electrical activity (top trace).

and maximal spike amplitude (27.3 ± 1.7 and 40.9 ± 2. mV, respectively) were significantly larger in Cx36$^{-/-}$ (n = 11; Table 1). To investigate the origin of this spike activity, Cx36$^{-/-}$ β-cells were voltage-clamped at −50 mV, as described above. Under these conditions, no inward current originating in neighboring cells could be observed (Fig. 6*B*). Spiking activity in β-cells of Cx36$^{-/-}$ mice was observed to cease within minutes. However, membrane potential remained at the threshold potential of about −40 mV and was not affected by the application of elevated glucose levels or tolbutamide with the perfusion (−38 ± 3 mV, n = 6). Furthermore, we were not able to detect bursting electrical activity in Cx36$^{-/-}$ β-cells.

The data are consistent with the view that, under resting conditions, β-cells control the electrical activity of their coupled neighbors by transmitting them through gap junctions, a current that prevents the potential to reach the threshold for activation of electrical activity. Necessarily, stimulation of the slices by glucose should be sufficient to circumvent this silencing effect of gap junctions. To test this implication, slices were preincubated for 7 min in the presence of 13 mmol/l glucose before recording. Under these conditions, the closure of K_{ATP} channels by ATP dialysis was followed by a rapid depolarization that reached the threshold potential, initially inducing a spike activity, which, in contrast to application of tolbutamide, turned into bursting after several minutes (Fig. 7). Continuous spiking activity lasted for 3–4 min and then turned into bursting activity. In all experiments, these oscillations were fast with a period of below 25 s throughout glucose administration (up to 6 min). After glucose removal, this electrical activity stopped, and the membrane potential hyperpolarized (Fig. 7) in a way similar to that observed after washout of tolbutamide (Fig. 4).

To further evaluate the influence of the membrane potential of individual β-cells on the electrical activity of their coupled neighbors, we simultaneously patch-clamped two coupled β-cells to record electrical activity of one cell while clamping the other to different membrane potentials. After blockade of K_{ATP} channels by dialysis of 5 mmol/l ATP and perfusion of the slices with 100 µmol/l tolbutamide, the membrane potential recorded from the first β-cell changed linearly, as a function of the potential imposed to the second cell (Fig. 8*A*). Additionally, the mean and maximal amplitude of spikes recorded in the first cell were reduced because of the hyperpolarization imposed to the second cell. The maximal amplitude decreased from 18.8 pA, when the second cell was clamped to −50 mV, to 10.4 pA at a clamp potential of −100 mV. As shown in Fig. 8*B*, the mean spike amplitude was significantly different at these two potentials (12.3 ± 0.4 and 8.0 ± 0.4 pA at −50 and −100 mV, respectively). However, whereas in some experiments an electrical activity was recorded in the first cell even when a major hyperpolarization was imposed to the second cell (Fig. 8), in others the spike activity stopped when the second cell was

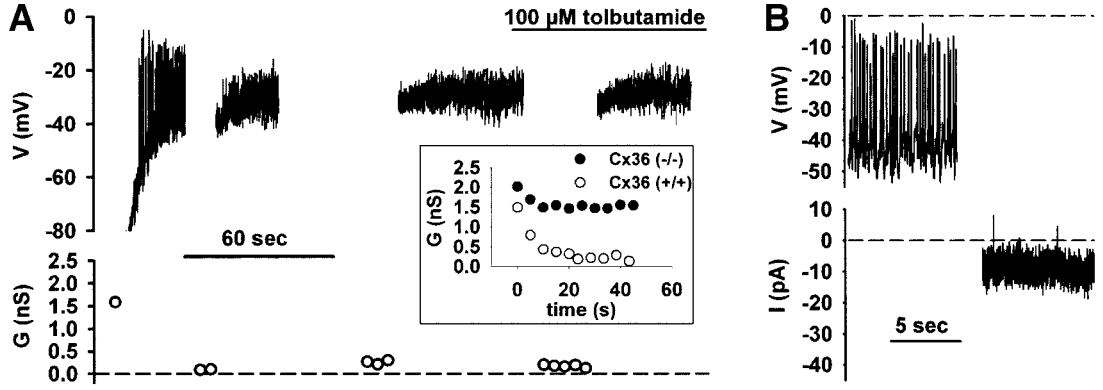

FIG. 6. Excitability of β-cells of Cx36$^{-/-}$ mice. *A*: Membrane potential (top trace) and whole-cell conductance (bottom trace) as a result of intracellular dialysis of 5 mmol/l ATP and extracellular application of 100 µmol/l tolbutamide. *Inset*: Closure of K_{ATP} channels by dialysis of 5 mmol/l ATP in β-cells of wild-type Cx36$^{+/+}$ and Cx36$^{-/-}$ mice in two experiments with comparable series resistance. *B*: Currents recorded at −50 mV (bottom trace) during electrical activity (top trace).

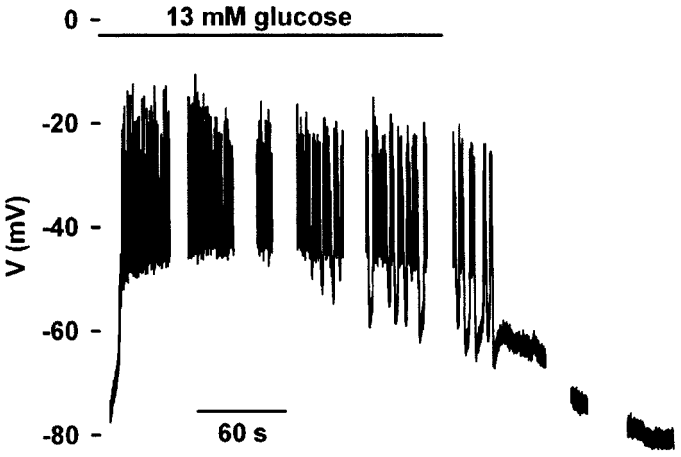

FIG. 7. Membrane potential changes after dialysis of 5 mmol/l ATP in a β-cell from Cx36$^{+/+}$ mice, after preincubation of the tissue slice in 13 mmol/l glucose for 7 min.

clamped at the resting potential value of −70 mV (data not shown).

Switching off insulin release was impaired in pancreata lacking Cx36. During the 15-min perfusion with 16.4 mmol/l glucose, the insulin release transiently increased during a 5-min-long first phase, which was followed by a sustained second-phase release period (12). When inflow of high glucose was abruptly discontinued and the perfusion system was switched to basal glucose levels, insulin release decreased exponentially with a time constant of 2.9 ± 0.0 min^{-1} and 3.1 ± 0.1 min^{-1} in Cx36$^{+/+}$ and Cx36$^{+/-}$, respectively (Fig. 9). In contrast, insulin release in Cx36$^{-/-}$ mice declined with a significantly longer time constant (17.3 ± 11.3 min^{-1}). In this experiment, the time axis also represents a decrease of glucose concentration, showing that β-cells lacking electrical coupling released insulin in response to a much wider glucose concentration range than cells coupled by Cx36 channels.

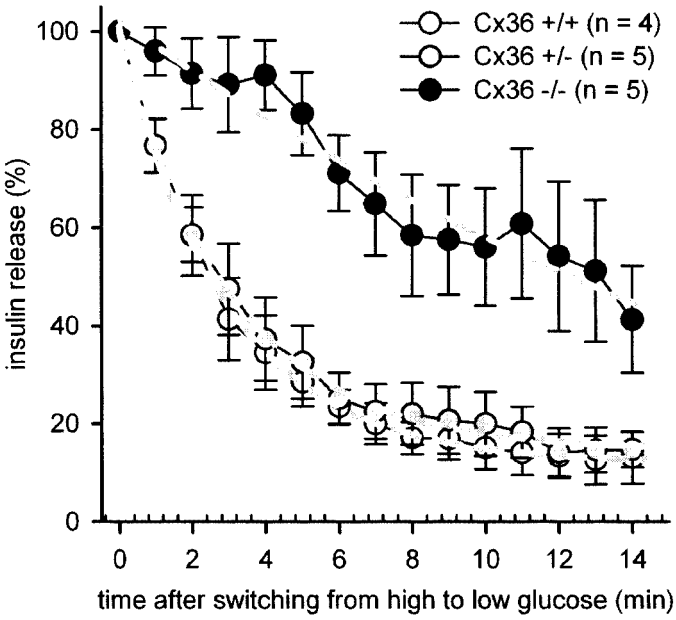

FIG. 9. Return of high glucose–stimulated insulin release to basal levels in perfused pancreas of wild-type and Cx36-deficient mice. Pancreata of Cx36$^{+/+}$ (open circles, n = 9) and Cx36$^{+/-}$ mice (gray solid circles, n = 10) showed an exponential decay of insulin output when glucose was switched from 16.4 to 1.4 mmol/l. In contrast, the decay in pancreata of Cx36 (−/−) mice (black solid circles, n = 10) was much more slow. Data are mean ± SE of four to five animals in each group.

DISCUSSION

We have compared the in situ electrophysiological properties of β-cells coupled by Cx36 channels with those of β-cells lacking this gap junction protein (12,13) using the recently developed pancreas slice model (14,15). Such a comparison was made possible inasmuch as β-cells of Cx36$^{+/+}$, Cx36$^{+/-}$, and Cx36$^{-/-}$ littermates had similar size and shape characteristics and a normal spatial distribution within the islets (12). Our work provides evidence that these cells are also comparable with regard to the main parameters that allow for an electrophysiological distinction between islet β-cells and non–β-cells (17), including capacitance values and membrane potential of the conditioning pulse, which reduces by one-half the Na^+ current. Also, the wild-type mice of the transgenic KOCx36 strain we used displayed most of the electrophysiological characteristics of control NMRI mice, which have so far been mostly used to investigate islet cell electrophysiology, including in terms of capacitance, membrane potential of the conditioning pulse V_h, and density of Ca^{2+} currents. Still, the two types of control animals had different residual conductances after blockade of K_{ATP} channels, suggesting different densities of gap junction channels. Furthermore, when studied without ATP in the pipette solution, the two types of mice also developed

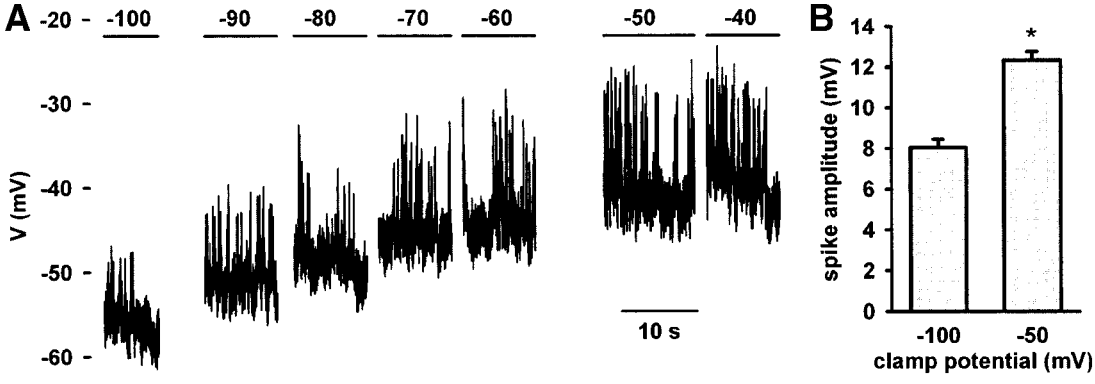

FIG. 8. Double patch-clamp experiment on two coupled β-cells within an islet of Langerhans of a Cx36$^{+/+}$ mouse. Electrical activity was induced by dialysis of both cells with 5 mmol/l ATP and perfusion of the tissue slice with 100 μmol/l tolbutamide. *A*: Membrane potential recording of one β-cell and its dependence on the membrane potential of the coupled β-cell. The coupled β-cell was clamped to the membrane potentials indicated on top of the graph. *B*: Average spike amplitude at different clamping voltages. *P < 0.001.

distinct maximal conductances, suggesting different densities of K_{ATP} channels. To prevent interference of these strain-dependent characteristics, all experiments compared β-cells of F5 $Cx36^{+/+}$, $Cx36^{+/-}$, and $Cx36^{-/-}$ littermates, which all had a similar, largely prominent C57Bl/6 genetic background (12).

Previously, it has been demonstrated that it is possible to estimate the gap junction conductance from the changes in holding current associated with the generation of electrical activity in the neighboring cells by using microelectrode recordings in islets of Langerhans (24,25). In our study, we assessed gap junction conductance using the whole-cell patch-clamp technique and manipulating K_{ATP}-channel activity, which has been shown to reveal similar values for coupling (17) and is independent from the status of the coupled cell. Comparison of $Cx36^{+/+}$ and $Cx36^{+/-}$ mice, which expressed Cx36, with $Cx36^{-/-}$ littermates that lacked this protein and gap junctions between β-cells (12), showed that the latter cells were fully electrically uncoupled, extending to current-carrying ions the conclusions previously reached using gap junction permeant tracers of larger size (12). Thus, the residual conductance measured in these mice (~0.2 nS) was similar to that observed in single β-cells. A major fraction of this conductance results from leak currents that, in this study, were not subtracted from recordings, because they did not interfere with β-cell excitability. A smaller fraction is probably also due to a negligible percentage of open K_{ATP} channels, and to other channels reported in β-cells (20). Interestingly, knocking out one allele of the Cx36 gene in $Cx36^{+/-}$ mice did not result in a significant decrease in gap junction conductance, in contrast to the decreased permeability observed after microinjection of Lucifer Yellow (12). This apparent discrepancy is likely related to the differential sensitivity of the electrophysiological and dye injection approaches, because the latter method tests the passage of tracers whose hydrated size is close to the estimated functional pore of the gap junction channels, whereas the first method uses the much smaller current-carrying ions. Although the previous study (12) and the present study concur to show that $Cx36^{+/-}$ mice were similar to controls with regard to insulin secretion, our novel data support the idea that electrical coupling is more important than metabolic coupling for such a controlled function (26,27). Cx36 forms gap junction channels with the lowest unitary conductance known to date and show no voltage sensitivity (21). Both features favor the use of Cx36 gap junctions as electrical couplers, which may account for the tissue distribution of this protein, which is restricted to pancreatic β-cells, adrenal medulla cells, and neurons (22). We were not able to confirm an effect of glucose on gap junctional coupling between β-cells (2), because long-term recordings of β-cells showed no change in residual conductance after exposure of stimulating concentrations of the sugar. We furthermore show here that Na^+-, K_v-, and K_{ATP}-channel densities are not affected by the knockout of one or two alleles of the Cx36 gene. In contrast, Ca^{2+} channels exhibit a significantly higher current density in mice lacking gap junctions, while retaining a similar kinetics and voltage dependence. It remains to be investigated whether this upregulation is a primary consequence of the knockout of the Cx36 gene or is a secondary effect of either compensatory mechanisms due to hyperexcitability or basal hyperinsulinemia (28). Furthermore, the physiological consequences of the Ca^{2+} conductance change remain to be established, as is the type of channels that mediate it. Further methodological refinements are required to make the pancreas slice preparation instrumental to address these questions.

To study the excitability of β-cells, we dialyzed the cytosol of individual cells with high ATP concentrations. A leak of the nucleotide into neighboring coupled cells that would result in a gradual depolarization of the membrane potential in the examined cell was not discovered, even in experimental recordings lasting for several tens of minutes.

Blockade of K_{ATP} channels in a single β-cell within an islet of Langerhans did not lead to electrical activity of this cell as long as the neighboring coupled cells were not stimulated. Although the mechanisms depolarizing membrane potential and inducing electrical activity were intact, the cell remained electrically silent and therefore presumably unable to secrete insulin. In contrast, in β-cells lacking Cx36, and therefore not coupled to neighboring cells, the closure of K_{ATP} channels suffices to depolarize the membrane to threshold potential and to induce electrical activity. Thus, under physiological conditions, the hyperpolarized membrane potential of unstimulated coupled neighbors clamps individual depolarized β-cells below the threshold potential for stimulation. Our interpretation is consistent with the recent report of a tight functional relationship between Cx36 channels and the Kir6.2-SUR1 complex of K_{ATP} channels able to balance for cell to cell variations (29), suggesting a mechanism whereby gap junctions prevent insulin secretion when only a few coupled β-cells are stimulated. When this effect of coupling is lost, the contribution of highly glucose-sensitive β-cells to insulin release is significantly enhanced. These results provide an explanation for the increased basal insulin release observed in Cx36-deficient mice (12), by demonstrating that gap junction coupling confines the concentration range of glucose that induces insulin secretion. In this way, the electrical coupling ensured by islet gap junctions also aligns the functional heterogeneity of β-cells (30–33). Thus, our study provides further support to the idea that coupling synchronizes β-cell activity as a function of the local glucose concentration (12) more than it propagates this activity into inactive regions of the islet (34). Our data further document that electrical coupling modulates the kinetics of insulin secretion. Thus, we have found that, after stimulation by high glucose, insulin secretion takes longer to return to basal levels in $Cx36^{-/-}$ mice than in heterozygous and wild-type littermates expressing Cx36, as also visible in a previous work (12). This effect can be ascribed to the fact that individual glucose-sensitive β-cells can no more be switched off by neighboring β-cells with a lower glucose sensitivity, because these cells are functionally isolated as a result of uncoupling. These findings experimentally validate in the intact pancreas some of the predictions made by mathematical modeling that electrical coupling should lead to a steeper, sigmoid-shaped glucose response, whereas uncoupling is expected to produce a more shallow and linear response (35). Hence, electrical coupling contributes to the control of blood glucose levels and may be particularly relevant to the prevention of hypoglycemic events, because of its ability to rapidly turn off the insulin output.

Using the whole-cell patch-clamp technique, the electrical activity recorded from gap junction–deficient β-cells runs down within minutes, whereas the membrane potential remains depolarized. Because stimulated Ca^{2+}-current amplitudes were also observed to run down to <20% of the

initial activity within 2–4 min (data not shown), a washout of cytosolic factors essential for Ca^{2+}-channel activity is presumably responsible for the cessation of the spiking activity. Therefore, and unlike the conclusions of an earlier study (14), the electrical activity recorded in the whole-cell mode after several minutes of dialysis originates from electrically coupled cells rather than from the patched β-cell itself. On the one hand, this conclusion stresses the limits of the whole-cell mode for long-time recordings of single cells and excludes the study of glucose sensitivity and other parameters affected by cytosolic washout of uncoupled cells. On the other hand, it demonstrates the possibility to use one β-cell as a biosensor to record the activity of the coupled islet network, because electrical coupling compensates for the heterogeneity of individual β-cells.

The oscillations of electrical activity that we recorded from wild-type β-cells were like the fast oscillations in membrane potential and [Ca^{2+}] previously published (36). Similar spike frequencies in coupled and noncoupled cells emphasize the intrinsic cellular mechanism underlying spiking and support our finding that channel kinetics are not altered by loss of Cx36. In contrast, the difference in spike amplitude may be due to several reasons, including the observed increase in Ca^{2+} current in the Cx36 knockout mice and, most likely, an effect of the higher membrane resistance of β-cells lacking gap junction channels.

It is not surprising that bursting electrical activity could not be recorded in the whole-cell patch-clamp mode from uncoupled β-cells of Cx36 knockout mice. As mentioned above, pipette dialysis leads to a rundown of Ca^{2+}-channel activity and to loss of metabolically derived oscillations in cytosolic ATP concentration within the patched cell, thus altering two cytosolic mechanism suggested to drive the bursts of electrical activity (37,38). However, under the same conditions, oscillations of electrical activity were readily detected in coupled β-cells after an initial phase of continuous spiking. Thus, even if an individual β-cell is continuously depolarized at threshold level, because of persistent closure of K_{ATP} channels, coupling to neighboring β-cells will force it to start oscillating. Therefore, our data experimentally documents how β-cell coupling can change a continuous depolarization into a bursting electrical activity, a concept that was so far postulated by mathematical modeling (35).

Clamping one β-cell to a hyperpolarized membrane potential results in the simultaneous hyperpolarization of both the patched and the nearby coupled β-cells. In some cases, electrical activity was still detectable in neighbors of β-cells clamped to extremely hyperpolarized membrane potentials, indicating that hyperpolarization of one cell is not sufficient to prevent the electrical activity of its coupled neighbors. However, in other recordings, the electrical activity was observed to stop in several cells after clamping one of them to resting membrane potential. These different reactions may depend on the location of the cells within the electrically active volume of the islet and on the extent of the coupling network. At any rate, these results indicate that silencing or activating a small percentage of β-cells in different islet regions has the potential of modulating the activity of the whole islet cells. This coordinated islet activity ensures that β-cells within an islet, and presumably also different islets within the pancreas, respond to a relatively narrow range of glucose concentrations. Such a response is required to obtain a pulsatile release of insulin from the pancreas (39), and the autonomic nervous system certainly plays a central role in this process (40–44). Thus, our observations raise the intriguing possibility that gap junction coupling not only synchronizes β-cells within individual islets of Langerhans, but also facilitates the synchronization of islets inside the pancreas by amplifying the effects of the islet innervation (45), which directly terminates on a limited number of endocrine cells (46). Whether a loss of Cx36-dependent signaling contributes in this manner to the development of a (pre-)diabetes state, as suggested in a recent work (12), remains to be fully ascertained in other animal models of the disease, such as those provided by the Zucker or the GK rats. At this time, no published work has reported on the levels of Cx36 expressed in these animals or on the function of the resulting cell-to-cell channels, and an interpretation of a change in such parameters should take into account the cell changes that inevitably take place during development of chronic hyperglycemia. Eventually, the recent finding that a chronic increase in glucose decreases Cx36 expression in vitro (47) suggests that the functions of β-cell coupling that we report here may be implicated in the impaired glucose-induced insulin secretion observed during the glucose desensitization and/or early glucotoxicity phenomena and may therefore be relevant to diabetes pathophysiology.

ACKNOWLEDGMENTS

S.S. has received European Commission Grant QLG1-CT-2001-02233. P.M. has received support from the Swiss National Science Foundation (310000-109402), the Juvenile Diabetes Research Foundation (1-2005-46, 1-2007-158), and the National Institutes of Health (RO1-DK-63443). M.R. has received European Commission Grant QLG1-CT-2001-02233. The European Neuroscience Institute Göttingen is jointly funded by the Göttingen University Medical School, the Max-Planck-Society, and Schering AG.

We thank Marion Niebeling and Heiko Röhse for excellent technical assistance.

REFERENCES

1. Orci L, Unger RH, Renold AE: Structural coupling between pancreatic islet cells. *Experientia* 29:1015–1018, 1973
2. Eddlestone GT, Goncalves A, Bangham JA, Rojas E: Electrical coupling between cells in islets of Langerhans from mouse. *J Membr Biol* 77:1–14, 1984
3. Michaels RL, Sheridan JD: Islets of Langerhans: dye coupling among immunocytochemically distinct cell types. *Science* 214:801–803, 1981
4. Meda P, Bosco D, Chanson M, Giordano E, Vallar L, Wollheim C, Orci L: Rapid and reversible secretion changes during uncoupling of rat insulin-producing cells. *J Clin Invest* 86:759–768, 1990
5. Valdeolmillos M, Santos RM, Contreras D, Soria B, Rosario LM: Glucose-induced oscillations of intracellular Ca2+ concentration resembling bursting electrical activity in single mouse islets of Langerhans. *FEBS Lett* 259:19–23, 1989
6. Pipeleers D, in't Veld PI, Maes E, Van De Winkel M: Glucose-induced insulin release depends on functional cooperation between islet cells. *Proc Natl Acad Sci U S A* 79:7322–7325, 1982
7. Serre-Beinier V, Le Gurun S, Belluardo N, Trovato-Salinaro A, Charollais A, Haefliger JA, Condorelli DF, Meda P: Cx36 preferentially connects β-cells within pancreatic islets. *Diabetes* 49:727–734, 2000
8. Theis M, Mas C, Doring B, Degen J, Brink C, Caille D, Charollais A, Kruger O, Plum A, Nepote V, Herrera P, Meda P, Willecke K: Replacement by a lacZ reporter gene assigns mouse connexin36, 45 and 43 to distinct cell types in pancreatic islets. *Exp Cell Res* 294:18–29, 2004
9. Calabrese A, Zhang M, Serre-Beinier V, Caton D, Mas C, Satin LS, Meda P: Connexin 36 controls synchronization of Ca2+ oscillations and insulin secretion in MIN6 cells. *Diabetes* 52:417–424, 2003
10. Caton D, Calabrese A, Mas C, Serre-Beinier V, Charollais A, Caille D,

Zufferey R, Trono D, Meda P: Lentivirus-mediated transduction of connexin cDNAs shows level- and isoform-specific alterations in insulin secretion of primary pancreatic beta-cells. *J Cell Sci* 116:2285–2294, 2003
11. Le Gurun S, Martin D, Formenton A, Maechler P, Caille D, Waeber G, Meda P, Haefliger JA: Connexin-36 contributes to control function of insulin-producing cells. *J Biol Chem* 278:37690–37697, 2003
12. Ravier MA, Guldenagel M, Charollais A, Gjinovci A, Caille D, Sohl G, Wollheim CB, Willecke K, Henquin JC, Meda P: Loss of connexin36 channels alters β-cell coupling, islet synchronization of glucose-induced Ca^{2+} and insulin oscillations and basal insulin release. *Diabetes* 54:1798–1807, 2005
13. Guldenagel M, Ammermuller J, Feigenspan A, Teubner B, Degen J, Sohl G, Willecke K, Weiler R: Visual transmission deficits in mice with targeted disruption of the gap junction gene connexin36. *J Neurosci* 21:6036–6044, 2001
14. Speier S, Rupnik M: A novel approach to in situ characterization of pancreatic beta-cells. *Pflugers Arch* 446:553–558, 2003
15. Speier S, Yang SB, Sroka K, Rose T, Rupnik M: K(ATP)-channels in beta-cells in tissue slices are directly modulated by millimolar ATP. *Mol Cell Endocrinol* 230:51–58, 2005
16. Charollais A, Gjinovci A, Huarte J, Bauquis J, Nadal A, Martin F, Andreu E, Sanchez-Andres JV, Calabrese A, Bosco D, Soria B, Wollheim CB, Herrera PL, Meda P: Junctional communication of pancreatic beta cells contributes to the control of insulin secretion and glucose tolerance. *J Clin Invest* 106:235–243, 2000
17. Gopel S, Kanno T, Barg S, Galvanovskis J, Rorsman P: Voltage-gated and resting membrane currents recorded from B-cells in intact mouse pancreatic islets. *J Physiol* 521:717–728, 1999
18. Barg S, Galvanovskis J, Gopel SO, Rorsman P, Eliasson L: Tight coupling between electrical activity and exocytosis in mouse glucagon-secreting α-cells. *Diabetes* 49:1500–1510, 2000
19. Gopel SO, Kanno T, Barg S, Rorsman P: Patch-clamp characterisation of somatostatin-secreting -cells in intact mouse pancreatic islets. *J Physiol* 528:497–507, 2000
20. Ashcroft FM, Ashcroft SJ, Harrison DE: Properties of single potassium channels modulated by glucose in rat pancreatic beta-cells. *J Physiol* 400:501–527, 1988
21. Srinivas M, Rozental R, Kojima T, Dermietzel R, Mehler M, Condorelli DF, Kessler JA, Spray DC: Functional properties of channels formed by the neuronal gap junction protein connexin36. *J Neurosci* 19:9848–9855, 1999
22. Al-Ubaidi MR, White TW, Ripps H, Poras I, Avner P, Gomes D, Bruzzone R: Functional properties, developmental regulation, and chromosomal localization of murine connexin36, a gap-junctional protein expressed preferentially in retina and brain. *J Neurosci Res* 59:813–826, 2000
23. Moreno AP, Berthoud VM, Perez-Palacios G, Perez-Armendariz EM: Biophysical evidence that connexin-36 forms functional gap junction channels between pancreatic mouse beta-cells. *Am J Physiol Endocrinol Metab* 288:E948–E956, 2005
24. Mears D, Sheppard NF Jr, Atwater I, Rojas E: Magnitude and modulation of pancreatic beta-cell gap junction electrical conductance in situ. *J Membr Biol* 146:163–176, 1995
25. Sherman A, Xu L, Stokes CL: Estimating and eliminating junctional current in coupled cell populations by leak subtraction: a computational study. *J Membr Biol* 143:79–87, 1995
26. Piston DW, Knobel SM, Postic C, Shelton KD, Magnuson MA: Adenovirus-mediated knockout of a conditional glucokinase gene in isolated pancreatic islets reveals an essential role for proximal metabolic coupling events in glucose-stimulated insulin secretion. *J Biol Chem* 274:1000–1004, 1999
27. Quesada I, Fuentes E, Andreu E, Meda P, Nadal A, Soria B: On-line analysis of gap junctions reveals more efficient electrical than dye coupling between islet cells. *Am J Physiol Endocrinol Metab* 284:E980–E987, 2003
28. Kato S, Ishida H, Tsuura Y, Tsuji K, Nishimura M, Horie M, Taminato T, Ikehara S, Odaka H, Ikeda I, Okada Y, Seino Y: Alterations in basal and glucose-stimulated voltage-dependent Ca2+ channel activities in pancreatic beta cells of non-insulin-dependent diabetes mellitus GK rats. *J Clin Invest* 97:2417–2425, 1996
29. Rocheleau JV, Remedi MS, Granada B, Head WS, Koster JC, Nichols CG, Piston DW: Critical role of gap junction coupled KATP channel activity for regulated insulin secretion. *PLoS Biol* 4:e26, 2006
30. Pipeleers D, Kiekens R, Ling Z, Wilikens A, Schuit F: Physiologic relevance of heterogeneity in the pancreatic beta-cell population. *Diabetologia* 37 (Suppl. 2):S57–S64, 1994
31. Heimberg H, De Vos A, Vandercammen A, Van Schaftingen E, Pipeleers D, Schuit F: Heterogeneity in glucose sensitivity among pancreatic beta-cells is correlated to differences in glucose phosphorylation rather than glucose transport. *EMBO J* 12:2873–2879, 1993
32. Herchuelz A, Pochet R, Pastiels C, Van Praet A: Heterogeneous changes in [Ca2+]i induced by glucose, tolbutamide and K+ in single rat pancreatic B cells. *Cell Calcium* 12:577–586, 1991
33. Salomon D, Meda P: Heterogeneity and contact-dependent regulation of hormone secretion by individual B cells. *Exp Cell Res* 162:507–520, 1986
34. Rocheleau JV, Walker GM, Head WS, McGuinness OP, Piston DW: Microfluidic glucose stimulation reveals limited coordination of intracellular Ca2+ activity oscillations in pancreatic islets. *Proc Natl Acad Sci U S A* 101:12899–12903, 2004
35. Smolen P, Rinzel J, Sherman A: Why pancreatic islets burst but single beta cells do not: the heterogeneity hypothesis. *Biophys J* 64:1668–1680, 1993
36. Bergsten P: Role of oscillations in membrane potential, cytoplasmic Ca2+, and metabolism for plasma insulin oscillations. *Diabetes* 51 (Suppl. 1):S171–S176, 2002
37. Kanno T, Rorsman P, Gopel SO: Glucose-dependent regulation of rhythmic action potential firing in pancreatic beta-cells by K(ATP)-channel modulation. *J Physiol* 545:501–507, 2002
38. Zhang M, Houamed K, Kupershmidt S, Roden D, Satin LS: Pharmacological properties and functional role of Kslow current in mouse pancreatic beta-cells: SK channels contribute to Kslow tail current and modulate insulin secretion. *J Gen Physiol* 126:353–363, 2005
39. Stagner JI, Samols E, Weir GC: Sustained oscillations of insulin, glucagon, and somatostatin from the isolated canine pancreas during exposure to a constant glucose concentration. *J Clin Invest* 65:939–942, 1980
40. Grapengiesser E, Dansk H, Hellman B: Pulses of external ATP aid to the synchronization of pancreatic beta-cells by generating premature Ca(2+) oscillations. *Biochem Pharmacol* 68:667–674, 2004
41. Hansen BC, Pek S, Koerker DJ, Goodner CJ, Wolfe RA, Schielke GP: Neural influences on oscillations in basal plasma levels of insulin in monkeys. *Am J Physiol* 240:E5–E11, 1981
42. Matthews DR, Lang DA, Burnett MA, Turner RC: Control of pulsatile insulin secretion in man. *Diabetologia* 24:231–237, 1983
43. Stagner JI, Samols E: Perturbation of insulin oscillations by nerve blockade in the in vitro canine pancreas. *Am J Physiol* 248:E516–E521, 1985
44. Sha L, Westerlund J, Szurszewski JH, Bergsten P: Amplitude modulation of pulsatile insulin secretion by intrapancreatic ganglion neurons. *Diabetes* 50:51–55, 2001
45. Meneghel-Rozzo T, Rozzo A, Poppi L, Rupnik M: In vivo and in vitro development of mouse pancreatic beta-cells in organotypic slices. *Cell Tissue Res* 316:295–303, 2004
46. Ushiki T, Watanabe S: Distribution and ultrastructure of the autonomic nerves in the mouse pancreas. *Microsc Res Tech* 37:399–406, 1997
47. Allagnat F, Martin D, Condorelli DF, Waeber G, Haefliger JA: Glucose represses connexin36 in insulin-secreting cells. *J Cell Sci* 118:5335–5344, 2005